In Vitro Mimicking the Morphology of Hepatic Lobule Tissue Based on Ca-Alginate Cell Sheets

Zeyang Liu,*[a] Minmin Lu,[a] Masaru Takeuchi,[a] Tao Yue,[c] Yasuhisa Hasegawa,[a] Qiang Huang[b] and Toshio Fukuda[ab]

Artificial cell sheets are commonly utilized as buiding blocks for tissue engineering. We propose a novel approach in the fabrication of Ca-alginate gel sheets, embedded with liver cells (RLC-18) in order to mimic liver lobule tissue. Ca-alginate sheets with hepatic lobule-shaped patterns were deposited onto a micro-electrode device using electrodeposition. Viability of embedded cells was ensured to exceed 80%. Cell morphology and biofunctionality were monitored during the one-week culture period and results compared with those of traditional 2D culture. In addition, we detached cell sheets from the electrode substrate and stacked them into a 3D multi-layered structure to mimic the morphology of liver lobule tissue.

Introduction

Various liver tissue engineering approaches currently under development, with applications ranging from artificial liver organ transplantation to cell-based therapies, rely on the ability to encapsulate hepatocytes in three-dimensional (3D) scaffolds. Hydrogels are attractive scaffolds for 3D cell culture and tissue engineering due to their tissue-like water content, injectability, and tunable properties. Extensive efforts have been made to allow the control of various hydrogel formations, such as thermoresponsive gel, photo-crosslinkable gel and chemical-crosslinkable gel; this control could facilitate drug release [1], cell assembly In vitro [2, 3], tissue formation [4-6] and subsequent transplantation [7].

A hydrogel made from an acidic polysaccharide of sodium alginate, which can ionically cross-linked with multivalent cations (e.g., Ca^{2+}, Fe^{3+}), is widely used to entrap and immobilize cells [8], as well as bacterial [9] and other bio-components. The "cell containing alginate hydrogel modules" take the form of cell droplets [10-13], cell microfibers [14, 15] and cell sheets [16, 17]. Challenges remain concerning the application of this hydrogel in tissue engineering; first, cell proliferation rate is slow within the gel due to a lack of cell adhesion molecules, although some researchers have indicated that the incorporation of RGD peptides can help cell adhesion [18]. Second, it is difficult to control the formation of a complex alginate hydrogel structure due to the diffusion of the multivalent cations in solution. Microfluidic technology and specialized devices with nozzle arrays are the common method to generate these structures [19-21].

Recently, electrodeposition has been well established [9, 22, 23]. This method is widely utilized to deposit alginate or chitosan gel film onto a specific area of 2D substrate for cell-cell signal studies [16, 24]. The mechanism of electrodeposition is used to release calcium ions from the region of the micro-electrode surface via electrolysis (H^+ is released from the anode and reacts with $CaCO_3$ particles to release calcium ions). Thus, these calcium ions can immediately react with alginate around the electrode to form an alginate hydrogel film. Simultaneously, bio-components are immobilized within the gel film for use in further applications [23]. The advantages of electrodeposition include the fact that the complex patterns to a resolution of <100 μm can be achieved [9]. Thus, this method successfully overcomes the shape control limitations of alginate gel. In our previous report [6], we demonstrated that issues with cell proliferation within alginate gel can be solved through an improved electrodeposition method which produces high cell-density microtissue. However, some challenges remain, limiting the use of electrodeposition in further applications of tissue engineering. Generally, the method restricts placement of fabricated alginate sheets to a 2D electrode. This limitation raises the question of whether the fabricated cell sheet could be detached and assembled for 3D tissue formation. In addition, the detached alginate sheets can curl themselves due to their flexibility and insufficiently cross-linked Ca-alginate structure [9], making them unsuitable building blocks for 3D stacking assembly. As a result, it is necessary to fabricate the gel sheet on a flat surface.

In the current study, we propose a method to fabricate Ca-alginate cell sheets for mimicking the morphology of hepatic lobule tissue based on the electrodeposition method. The

[a] *Department of Micro-Nano Systems Engineering, Nagoya University, Furo-cho, Chikusa-ku, Nagoya, 464-8603, Japan. E-mail: liu@robo.mein.nagoya-u.ac.jp; Tel: +81 52 789 4481.*
[b] *Intelligent Robotics Institute, School of Mechatronical Engineering,Beijing Institute of Technology, Key Laboratory of Biomimetic Robots and Systems, Ministry of Education of China, 5 South Zhongguancun Street, Haidian District, Beijing, 100081, China.*
[c] *Department of Biomedical Engineering, University of California, Irvine, 3120 Natural Sciences II Irvine, CA 92697-2715, USA.*
† Electronic Supplementary Information (ESI) available: See

centimeter-scale cell sheets were produced with pre-designed hepatic lobule patterns. After a one-day culture, we successfully detached the sheets from the 2D electrode substrate without any structural defect and stacked them into 3D multilayered liver lobule structure within a PDMS mold. Cell proliferation and functionality of the fabricated Ca-alginate cell sheet were quantitatively compared to that of regular 2D culture. This study aims to clarify that alginate cell sheets created by electrodeposition can potentially be utilized for 3D tissue constructs. A research map is shown in Fig. 1.

This work is potentially significant for a number of reasons. First, we demonstrate that alginate sheet fabrication with hepatic lobule patterns using electrodeposition can be potentially utilized for 3D tissue constructs. Second, an easy method is proposed to detach the sheet from a flat surface without any defect. We also show that the detached sheets can be transferred simply using a 1-ml pipette, then stacked into a multi-layered tissue. We believe our method provides a suitable platform for constructing a 3D cell model by stacking alginate cell sheets using electrodeposition. This platform has the potential to uncover new uses for electrodeposition in various applications such as in cell–ECM interactions, structure–function relationships, tissue morphogenesis, and modular tissue reconstructions.

Materials and methods

2.1 Materials and solution preparation

We used sodium alginate (Medium viscosity, A2033), fluorine doped tin oxide coated glass slide (surface resistivity ~7 Ω/sq, 735140) (Sigma-Aldrich) and HEPES (346-01373) (Wako Pure Chemical Industries). Calcium carbonate ($CaCO_3$) (0.97 µm, #2300) were kindly supplied from Sankyo-seifun Ltd (Japan). Photoresist (AZ5214-E) were purchased from AZ electronic material GmbH. Cell Counting Kit-8 (CCK8) was purchased from Dojindo Ltd (Japan). Rat albumin enzyme-linked immunosorbent assay (ELISA) Quantitation kit (ERA3201-1) was purchased from Assaypro Inc (USA). The water used to prepare the solution was deionized with a Millipore Direct-Q3 water purification system (Millipore, Worcester, MA).

2.1.1. Deposition solution

The deposition solution was prepared by dissolving 1% w/v alginate sodium in solution containing NaCl (126 mM), KCl (2.7 mM), $Na_2HPO_4{\cdot}12H_2O$ (8.1 mM), KH_2PO_4 (1.47 mM) and HEPES (21 mM). The pH was adjusted to 7.3 by adding 0.5M NaOH solution. $CaCO_3$ (0.5% w/v) was uniformly dispersed in the solution using magnetic stirrer for 24h.

2.1.2. HEPES buffer solution

The HEPES buffer solution was prepared by dissolving HEPES (5g/L) in solution containing NaCl (8 g/L), KCl (0.37 g/L), Na_2HPO_4 (1.076 g/L) and glucose (1 g/L). pH was adjusted to 7.3 by adding 0.5M NaOH solution.

2.1.2. Calcium chloride solution

To prepare 1.1% calcium chloride solution, 0.55 g of $CaCl_2$ (anhydrous) is dissolved in 50 ml of distilled water.

2.1.5. Cell viability test solution

The cell viability solution was a mixture of 0.8 µL calcein AM (1 mg/mL, Wako), 2.8 µL propidium iodide (PI) (1 mg/mL, Wako) and 1 mL HEPES buffer solution.

2.2 Fabrication of micro-patterned electrode

The photolithographic technique was used to construct the electro-device in this experiment. Briefly, fluorine-doped tin oxide (FTO) glass slides (2.5 cm × 5 cm) were washed with isopropyl alcohol and Milli-Q water using an ultrasonic cleaner. The photoresist (AZ 5214E) was coated onto the surface of FTO glass with 1.4-µm thickness.

The micro-patterns were designed to mimic liver lobule morphology as shown in Fig. 1A. The length of the sheet is 1.2 cm and the width is 0.95 cm. There are two types of hepatic lobule pattern utilized in the current work: one with a diameter of 1.5 mm and the other of 2 mm. The hepatic lobule is a building block of the liver consisting of a portal triad, hepatocytes arranged in linear cords between a capillary network (hepatic sinusoid), and a central vein. The peculiarity of liver sinusoids consists in the fact that blood infuses the liver lobule unidirectionally, entering the portal area and ending its pathway in the central vein. When compared with liver histology, the circular hole of the micro-pattern mimics the central vein. Around the central vein, eight ellipsoidal holes represent hepatic sinusoids as communication paths between the portal vessels and central vein. The other area on the alginate sheet embedded with hepatic cells mimics the hepatic cord. The patterned-electrode was fabricated using a laser writing device (µPG 101, Heidelberg, German) based on our AutoCAD design of micro-electrodes.

2.3 Cell culture

Rat liver (RLC-18) cells were cultured for experiments with Dulbecco's modified Eagle's medium (DMEM) supplemented with 10% fetal bovine serum (FBS) and 1% penicillin streptomycin in a 10-cm tissue culture dish at 37 °C in a humidified 5% CO_2 incubator. When reaching 90% confluence, cells were detached using trypsin/EDTA (Invitrogen) and gently pipetted to break aggregates. The cells were then centrifuged, re-suspended, and counted for further passaging or experimental use.

2.4 Electrodeposition of Ca-alginate gel sheet

To fabricate the Ca-alginate gel sheet with hepatic lobule patterns using the electrodeposition method, the following steps were performed:

1) The prepared RLC-18 cells were centrifuged and washed with HEPES buffer twice to fully remove the culture medium since

the DMEM may interfere with the electrodeposition chemical reaction and generate bubbles. Then, 700 µl deposition solution was mixed with the centrifuged RLC-18 cells by gently pipetting.

2) 500 µl deposition solution was taken from the mixed 700 µl cell deposition solution to be placed onto the electrode area, as shown in figure 1B.

3) A DC power supply was connected to the device using two copper wires. One copper wire was immersed into the deposition solution as a cathode at a depth of about 1 mm. The other copper wire was attached to the surface of the FTO glass as an anode.

4) A DC voltage was applied to the FTO electrode to trigger electrolysis and start the electro-deposition process. The Ca-alginate gel sheet was deposited onto the patterned electrode area based on the electrodeposition principle as shown in Fig. 2A.

5) After 15 s, the DC power supply was turned off immediately and extra non-cross-linked alginate solution was removed by a pipette. Then, the FTO glass was transferred into HEPES solution for washing.

6) The FTO glass was gently shaken for several minutes until the boundary of the hepatic lobule pattern on the gel sheet could be clearly identified under an optical microscope.

2.5 Detachment of the fabricated gel sheet from the substrate

The detachment method process is shown in Fig. 3A. After washing (see '5)' above), 1.1% $CaCl_2$ solution was dropped onto the gel sheet for 15 min; Ca^{2+} ions harden the gel structure by cross-linking with alginate chains. The $CaCl_2$ solution was then removed and the FTO glass immersed in HEPES solution or DMEM solution (the latter if using cells) at 37 °C in a humidified 5% CO_2 incubator. After 24 h, the gel sheet detached from the FTO glass substrate automatically.

2.6 Viability assay for RLC-18 cells within alginate sheets

In order to confirm whether the presented method is suitable for use in biological applications, cell viability of the fabricated alginate sheet was checked soon after electrodeposition and on day 4 of the culture period. The fabricated structures were washed once with HEPES buffer solution and then immersed into the cell viability test solution for 30 min in an incubator. Then, the structures were washed with HEPES buffer solution again. A fluorescence microscope was used to observe the samples. Cell viability was measured by calculating the viable and dead cells in each frame.

2.7 Cell number counting

Cell Counting Kit-8 (CCK8) was utilized to measure the cell number of fabricated alginate sheets and a 2D culture control group. CCK8 is sensitive in the detection of viable cells similar to other tetrazolium salts such as MTT and MTS. We constructed the calibration curve based on the relationship between the known cell number and absorbance value. The procedure for cell counting involved: 1) Incubation of individual sheet or diluted cell suspension of 2D culture (100 µl/well) in a 96-well plate. 2) Adding 10 µl of the CCK8 solution to each well of the plate. 3) Incubating the plate for 3 h in the incubator. 4) Immediately measuring absorbance at 450 nm using a microplate reader (Infinite F50 plate readers, TECAN) to determine the cell number of each microtissue.

2.8 Albumin secretion assay

A rat albumin ELISA quantitation kit was used to measure albumin levels during the culture period (at 1, 2, 3, 4 and 5 days). Before the assay, the fabricated alginate sheets were washed with PBS and fresh medium was added; after 24 h, this medium was withdrawn and aliquots were temporarily stored at -20 °C. The levels of albumin measured at each time point were normalized to each dish or the cell number.

2.9 Assembly of 2-layered hepatic lobule-like tissue within a PDMS mold

The ability to generate 3D multilayered cellular hydrogel structures is critical to the engineering of spatially complex liver tissues. Thus, we performed a simple experiment to demonstrate that reliable handling and assembly techniques, including cell sheet detachment, transfer and stacking, were applied in our method. We used a modified method here based on W. Lee's work [25]. Briefly, the detached cell sheets were collected using a modified pipette in a randomly folded configuration. The folded cell sheet spontaneously unfolded when released into the PDMS mold. The transferred cell sheets sank to the bottom of the PDMS mold when aspirating the surrounding medium. The transfer and stacking steps were repeated to assemble multi-layered hepatic lobule-like tissue. The dimension of the PDMS mold was designed to fit the size of the fabricated cell sheet to maximize the alignment resolution.

2.10 Detection and analysis System

The Ca-alginate gel structures and alginate-PLL microcapsules were observed under a microscope (IX81, Motorized Inverted Research Microscope with confocal system, Olympus, Germany) in both bright field and fluorescence modes. Images were captured using the CCD camera on the microscope. We used image analysis software ImageJ (ImageJ 1.47v, National Institutes of Health, USA) to analyze the characteristics of the microcapsules through the images.

2.11 Statistical analysis

Values are expressed as mean ± standard deviation (SD). Where appropriate, the two-tailed student's *t*-test was used to determine statistical differences between groups. A p-value of less than 0.05 was considered statistically significant.

3. Results and discussion

3.1 Electrodeposition of Ca-alginate gel sheet

Before the experiment, the deposition solution was stirred again to evenly disperse the $CaCO_3$ particles and heated to 37 °C. In the meantime, 1 ml of the pre-prepared RLC-18 cell suspension (cell concentration: 10^7 cells/ml) was centrifuged and washed with phosphate-buffered saline (PBS) twice to remove the DMEM, which might have interfered with the electrodeposition reaction. The cell suspension was then centrifuged again, mixed with 700 µL of the heated deposition solution, and evenly dispersed by gently pipetting. Finally, 500 µL of the 700 µL deposition solution was dropped onto the microelectrode area as shown in Fig. 2B.

A DC voltage of 4.63 v was applied for 15 s to trigger the electrodeposition process. The concept of the electrodeposition principle is shown in Fig. 2A. Briefly, H^+ is generated by the electrolysis of water formed in an acidic microenvironment at the anode surface ($2H_2O \rightarrow O_2+4H^++4e^-$). Ca^{2+} is released from $CaCO_3$ particles as they encounter protons at the anode ($2H^++CaCO_3 \rightarrow Ca^{2+}+H_2O+CO_2$). The calcium alginate hydrogel films are formed when calcium ions cross-link with alginate immediately ($Ca^{2+}+2Alg\text{-}COO^- \rightarrow Alg\text{-}COO^-\text{-}Ca^{2+}\text{-}OOC\text{-}Alg$). Therefore, the shape of the gel sheet can be altered by changing the design of the micro-electrode.

Figure 2C shows the fabricated Ca-alginate gel sheet after washing with HEPES solution for 2 min. In Fig. 2D, we show cases where a lower voltage was used, which leads to unstable gel sheet generation due to insufficient cross-linking of Ca-alginate chains; and cases where a higher voltage was used which leads to generation of a thick gel sheet without the hepatic lobule pattern due to the diffusion of Ca^{2+} ions.

3.2 Detachment of the fabricated gel sheet from the substrate

Figure 3A shows the detachment procedure of the fabricated gel sheet from the FTO glass substrate. As described in the previous section, the gel sheet was fabricated onto the micro-electrode (Fig. 3AII). Then, 1.1% $CaCl_2$ solution was dropped onto the gel sheet to harden the gel structure (Fig. 3AIII). After 15 min, the $CaCl_2$ solution was removed and the FTO glass with the gel sheet was immersed in the culture medium for further incubation. After 24 h, the gel sheet can be easily detached from the FTO glass by shaking (Fig. 3AIIII). Without the 24-h incubation, it is difficult to detach the gel sheet without any defect either by shaking or pipetting. The fabricated gel sheet will strongly adhere to the FTO glass after $CaCl_2$ treatment due to surface tension.

In fact, we have tried several methods to detach the fabricated gel sheets, including:

1) As we described above, treating the fabricated gel sheet with $CaCl_2$ and culturing within DMEM for 24 h. Then, the gel sheet can be detached simply and easily by shaking the dish. This is the recommended method.

2) Detaching the gel sheet soon after electrodeposition without $CaCl_2$ treatment. The gel sheet can be detached simply by shaking. However, the detached gel sheet will curl itself automatically with or without the later $CaCl_2$ treatment.

3) Treating the fabricated gel sheet with $CaCl_2$ and starting the detachment immediately. The gel sheet can be detached by gently pipetting. The video of this detachment process can be found in the supplementary material. This method requires more than 2 min to detach one gel sheet. In addition, pipetting may bring damage to the gel sheet, which leads to a structure defect.

4) Treating the fabricated gel sheet with $CaCl_2$ and then immersing the sheets into cell viability test solution for 30 min. The gel sheet can be easily detached by shaking. A possible reason is that the Calcein-AM and PI are capable of weakening the Calcium-alginate chain. However, the PI may have a poisonous effect on cells.

Another possible solution to the detachment issue is to treat the FTO glass with oxygen plasma to make the surface hydrophilic. However, after O_2 plasma treatment, we found that the dropped deposition solution spread all over the FTO surface instead of remaining within the micro-electrode area.

The fabricated gel sheet before and after detachment is shown in Fig. 3B and Fig. 3C, respectively. Fluorescence beads were utilized to replace the liver cell to demonstrate the fabricated hepatic lobule patterns. To eliminate the effect of fluorescence beads on the results of electrodeposition in relation to the measurements and errors, carboxylate microspheres with small diameter (0.5 µm) were prepared to replace cells. According to our experimental data, we found that the fluorescence beads have no effect on the Ca-alginate electrodeposition. The hepatic lobule pattern with a 1.5 mm diameter was imaged using fluorescence microscopy before and after detachment (Fig. 3BII and 3CII respectively). The results corresponding to the 1.5 mm diameter were measured to be 1567 $\pm$ 133 µm in diameter ($n > 10$). The hepatic lobule pattern with 2 mm diameter was imaged using fluorescence microscopy before and after the detachment (Fig. 3BIII and Fig. 3CIII respectively). The results corresponding to the 2 mm diameter were measured to be 2028 $\pm$ 61 µm in diameter ($n > 4$). The shape and size of the fabricated hepatic lobule pattern were as same as the initial electrode design as shown in Fig. 3A. Therefore, the proposed method has the advantage of allowing fabrication of the flat Ca-alginate gel sheet with a precise predesigned micro-pattern and flat surface. Compared with the common alginate gel containing cell module, e.g., alginate droplet [11], alginate fiber [15] and Ca-alginate 3D printing system [26], the current study proposes an alternative

way to fabricate 2D alginate gel sheet for 3D complex tissue constructs in the tissue engineering field.

3.3 Evaluation of cell viability and thickness of the gel sheet

Figure 4A shows the optical and fluorescence microscopy images of cell viability soon after the electrodeposition process. RLC-18 cells were entrapped within the Ca-alginate hydrogel and assayed using the live/dead kit. By calculating the number of live and dead cells (green and red respectively), the cell viability was measured to be ~80%.

Figure 4B shows the 3D image of the fabricated alginate sheet under 3D laser confocal microscope. The RLC-18 cells were replaced by fluorescent beads for laser scanning. The thickness of the alginate sheet was approximately 302 $\pm$ 22 μm (N>3).

Figure 4C shows the cell viability after Ca^{2+} treatment (time 0 of the culture), Day 1, Day 4 and Day 10. There is no significant change in cell viability during Day 0, Day 1 and Day 4. Cell viability of Day 10 was significantly upregulated compared with the one of Day 4. The possible reason is that the cells within alginate hydrogel kept proliferating and started to form cell aggregates during the culture period. On the other hand, most of cells were maintained to be alive thanks to the bio-combability of the alginate hydrogel. Optical and fluorescence images of the RlC-18 cell morphology within Ca-alginate sheet after $CaCl_2$ treatment and cultured for 10-days were shown in Figure S1 and S2 respectively.

3.4 Cell number counting

Figure 5A shows the calibration curve of a linear-fitting model generated by the known cell number. Figure 5B shows the cell number of alginate sheet and 2D culture groups during the incubation period (day 1, 2, 3, 4 and 5).

RLC-18 cells within the alginate sheets had an initial cell number of ~$6*10^4$ cells and finally reached ~$25*10^4$ cells on day 5, a four-fold increase. On the other hand, the RLC-18 2D culture group increased from an initial ~$5*10^4$ cells to ~$133*10^4$ cells on day 5 – a 25-fold increase.

From the results, we believe the cells entered the logarithmic phase from day 3, resulting in an increase in cell proliferation. However, on day 3, cell proliferation rate within the alginate sheets is still slow even after entering the logarithmic phase. Other researchers also found this phenomenon, indicating the lack of adherence molecules inside the hydrogel as a major reason [27]. Recently, this issue was countered by incorporation of RGD peptides [28] and microcapsule technique to promote cell proliferation [29].

3.4 Albumin secretion

The purposes of measuring the albumin secretion here include the fact that albumin is considered an important feature of well-differentiated hepatocytes, and that cells cultured within alginate sheets may have an advantage over conventional 2D culture in terms of biofunctionality.

Figure 6A shows the albumin secretion per dish of the alginate sheets and 2D culture. Albumin secretion showed an increasing trend during 5-days culture because the cell number is increasing. Initially, albumin secretion from alginate sheets was almost the same as that seen in 2D culture, but from day 3, the albumin secretion of the latter was significantly higher than that of the alginate sheets, and was 2.6 times higher on day 5 (p = 0.01616, n = 4). A possible explanation of this phenomenon is that cell proliferation in 2D culture was higher than that of the Ca-alginate, as shown in Figure 5B.

Figure 6B shows the albumin secretion per 100 cells of the RLC-18 alginate sheets and 2D culture. The cells within the alginate gel showed a significantly higher albumin activity than cells cultured in 2D shapes and reached a maximum value at day 3. This result indicates that the cells growing in 3D culture dramatically increase their activity and regain biofunctionality. Usually, peak albumin secretion coincides with cell confluence, which is also characterized by decreased cell proliferation. The peak albumin secretion in Fig. 6B also suggests that the cells entered the logarithmic phase of proliferation on day 3. During the culture periods, the hepatocytes showed appreciable levels of albumin secretion ~6-12 pg/10^2 cells compared with that of 0-6 pg/10^2 cells under 2D culture. This result is consistent with a report that the 3D hepatocytes micro-organoids are critical for preserving hepatocyte function and other three-dimensional systems [14, 30].

3.5 Assembly of 2-layered hepatic lobule-like tissue

Figure 7A shows the results of cell sheets embedded with hepatic cells before assembly. On day 1, the deposited alginate gel structures were imaged and incubated. On day 3, before detachment, the cells started to adhere onto the bare area of the FTO glass surface. After detachment, hepatic lobule patterns were preserved without any defect while embedded with RLC-18 liver cells. Here, we used a high initial cell density (10^7 cells/ml in deposition solution) to address the cell proliferation issue within the alginate gel. On day 4, we collected the cell sheet and further transferred them into the PDMS mold for assembly layer by layer. By day 6, the hepatic cells merged together to mimic the hepatic cord while the ellipsoidal holes could still be clearly identified.

Figure 8 shows the additional experiment for confirmation of the hepatic lobule patterns alignment after the stacked assembly. Alginate sheets containing liver cells were assembled into a pre-defined PDMS mode layer by layer to form a 2-layered hepatic lobule structure as we mentioned above. The optical and fluorescence images of 1st layer and 2nd layer were obtained by only adjusting the Z position of the microscope respectively. The results show that the patterns were aligned

during stacking to form an uninterrupted central vein. The alignment error is less than 200 µm. Therefore, the proposed method provides a suitable and easy approach for mimicking the morphology of the hepatic lobule-like tissue.

The purpose of assembling the alginate sheets into a multi-layered structure was to demonstrate the feasibility of the method in fabricating a 3D cell model such as mimicking the morphology of the hepatic lobule-like tissue by using alginate cell sheets as building blocks. When compared to similar work , our method differs from that used by Je-kyun Park's group [25] with respect to the improved electrodeposition method used for the fabrication of precise and shape-controlled micro-patterns; and from that used by Tomokazu Matue's group [16] with respect to the movability of the detached flat cell sheet for further 3D tissue formation. In addition, our method shows advantages of micro-level high resolution and simplicity compared with commonly utilized 3D alginate cell-containing fiber printing techniques for 3D tissue reconstruction [26, 31]. Although the current fabricated structure only mimics the morphology of the hepatic lobule tissue because it cannot be perfused. However, the holes in the sheets are useful in ensuring proper exchange of oxygen, nutrients, and catabolites between cells and culture medium; thus, we believe, the construct may offer considerable benefits in terms of survival and functional performance. Therefore, the proposed technique has the potential for the design of three-dimensional lobule-like constructs by stacking varying deposited alginate sheets with complex micro-patterns and different cell lines for further applications in tissue engineering.

Conclusion

In summary, this paper presents a method for the fabrication of Ca-alginate cell sheets as building blocks for mimicking the morphology of hepatic lobule tissue. The alginate RLC-18 cell sheets with hepatic lobule micro-patterns were first deposited onto an electrode surface based on the electrodeposition method. After a one-day culture, the RLC-18 cells sheets were detached from 2D substrate and further assembled into a pre-designed PDMS mold. The fabricated cell sheets can be easily transferred by a 1 ml pipette and stacked layer by layer to mimic the morphology of hepatic lobule tissue. The developed method provides a new "bottom-up" paradigm to build 3D macroscopic liver tissue similar to that in vivo. The assembled hepatic lobule structure holds great promise to be improved further as in vitro models of liver organs and promote the novel applications of electrodeposition methods in tissue engineering.

Acknowledgment

This work was supported in part by the Ministry of Education, Culture, Sports, Science and Technology of Japan (Grants-in-Aid for BioAssembler (23106006)).

References

[1] X.-H. Ge, J.-P. Huang, J.-H. Xu, and G.-S. Luo, "Controlled stimulation-burst targeted release by smart decentered core–shell microcapsules in gravity and magnetic field," *Lab Chip,* vol. 14, pp. 4451-4454, 2014.

[2] M. Takeuchi, M. Nakajima, M. Kojima, and T. Fukuda, "Handling of micro objects using phase transition of thermoresponsive polymer," *Journal of Micro-Bio Robotics,* vol. 8, pp. 53-64, 2013.

[3] H. Wang, Q. Huang, Q. Shi, T. Yue, S. Chen, M. Nakajima*, et al.*, "Automated assembly of vascular-like microtube with repetitive single-step contact manipulation," *Biomedical Engineering, IEEE Transactions on* vol. VOL. 62, NO. 11, 2015.

[4] T. Yue, M. Nakajima, M. Takeuchi, C. Hu, Q. Huang, and T. Fukuda, "On-chip self-assembly of cell embedded microstructures to vascular-like microtubes," *Lab on a Chip,* vol. 14, pp. 1151-1161, 2014.

[5] K. Dubbin, Y. Hori, K. K. Lewis, and S. C. Heilshorn, "Dual‐Stage Crosslinking of a Gel‐Phase Bioink Improves Cell Viability and Homogeneity for 3D Bioprinting," *Advanced healthcare materials,* vol. 5, pp. 2488-2492, 2016.

[6] Z. Liu, M. Takeuchi, M. Nakajima, Y. Hasegawa, Q. Huang, and T. Fukuda, "Shape-controlled High Cell-density Microcapsules by Electrodeposition," *Acta Biomaterialia,* 2016.

[7] H. Onoe, T. Okitsu, A. Itou, M. Kato-Negishi, R. Gojo, D. Kiriya*, et al.*, "Metre-long cell-laden microfibres exhibit tissue morphologies and functions," *Nature Materials,* vol. 12, pp. 584-590, Jun 2013.

[8] S.-H. Huang, H.-J. Hsueh, and Y.-L. Jiang, "Light-addressable electrodeposition of cell-encapsulated alginate hydrogels for a cellular microarray using a digital micromirror device," *Biomicrofluidics,* vol. 5, p. 034109, 2011.

[9] Y. Cheng, C. Y. Tsao, H. C. Wu, X. Luo, J. L. Terrell, J. Betz*, et al.*, "Electroaddressing functionalized polysaccharides as model biofilms for interrogating cell signaling," *Advanced Functional Materials,* vol. 22, pp. 519-528, 2012.

[10] P. Agarwal, S. Zhao, P. Bielecki, W. Rao, J. K. Choi, Y. Zhao*, et al.*, "One-step microfluidic generation of pre-hatching embryo-like core–shell microcapsules for miniaturized 3D culture of pluripotent stem cells," *Lab on a Chip,* vol. 13, pp. 4525-4533, 2013.

[11] H. Hirama, T. Kambe, K. Aketagawa, T. Ota, H. Moriguchi, and T. Torii, "Hyper alginate gel microbead formation by molecular diffusion at the hydrogel/droplet interface," *Langmuir,* vol. 29, pp. 519-524, 2013.

[12] S. Zhao, P. Agarwal, W. Rao, H. Huang, R. Zhang, Z. Liu*, et al.*, "Coaxial electrospray of liquid core–hydrogel shell microcapsules for encapsulation and miniaturized 3D culture of pluripotent stem cells," *Integrative Biology,* vol. 6, pp. 874-884, 2014.

[13] C. Kim, S. Chung, Y. E. Kim, K. S. Lee, S. H. Lee, K. W. Oh*, et al.*, "Generation of core-shell microcapsules with three-dimensional focusing device for efficient formation of cell spheroid," *Lab on a Chip,* vol. 11, pp. 246-252, 2011.

[14] M. Yamada, R. Utoh, K. Ohashi, K. Tatsumi, M. Yamato, T. Okano*, et al.*, "Controlled formation of heterotypic hepatic micro-organoids in anisotropic hydrogel microfibers for long-term preservation of liver-specific functions," *Biomaterials,* vol. 33, pp. 8304-8315, Nov 2012.

[15] Y. Sequential assembly of cellZuo, X. He, Y. Yang, D. Wei, J. Sun, M. Zhong*, et al.*, "Microfluidic-based generation of functional microfibers for biomimetic complex tissue construction," *Acta biomaterialia,* vol. 38, pp. 153-162, 2016.

[16] K. Ino, T. Arai, J. Ramón-Azcón, Y. Takahashi, H. Shiku, and T. Matsue, "Alginate gel microwell arrays using electrodeposition for three-dimensional cell culture," *Lab on a Chip,* vol. 13, pp. 3128-3135, 2013.

[17] X. W. Shi, C. Y. Tsao, X. Yang, Y. Liu, P. Dykstra, G. W. Rubloff*, et al.*, "Electroaddressing of Cell Populations by Co‐Deposition with Calcium Alginate Hydrogels," *Advanced Functional Materials,* vol. 19, pp. 2074-2080, 2009.

[18] F. Yang, C. G. Williams, D.-a. Wang, H. Lee, P. N. Manson, and J. Elisseeff, "The effect of incorporating RGD adhesive peptide in polyethylene glycol diacrylate hydrogel on osteogenesis of bone marrow stromal cells," *Biomaterials,* vol. 26, pp. 5991-5998, 2005.

[19] S. Sugiura, T. Oda, Y. Aoyagi, M. Satake, N. Ohkohchi, and M. Nakajima, "Tubular gel fabrication and cell encapsulation in laminar flow stream formed by microfabricated nozzle array," *Lab Chip,* vol. 8, pp. 1255-1257, 2008.

[20] N. A. Raof, M. R. Padgen, A. R. Gracias, M. Bergkvist, and Y. Xie, "One-dimensional self-assembly of mouse embryonic stem cells using an array of hydrogel microstrands," *Biomaterials,* vol. 32, pp. 4498-4505, 2011.

[21] S.-Y. Teh, R. Lin, L.-H. Hung, and A. P. Lee, "Droplet microfluidics," *Lab on a Chip,* vol. 8, pp. 198-220, 2008.

[22] Y. Cheng, X. L. Luo, J. Betz, G. F. Payne, W. E. Bentley, and G. W. Rubloff, "Mechanism of anodic electrodeposition of calcium alginate," *Soft Matter,* vol. 7, pp. 5677-5684, 2011.

[23] Z. Liu, M. Takeuchi, M. Nakajima, C. Hu, Y. Hasegawa, Q. Huang*, et al.*, "Three-dimensional Hepatic Lobule-like Tissue Constructs Using Cell-microcapsule Technology," *Acta Biomaterialia,* 2016.

[24] S.-H. Huang, L.-S. Wei, H.-T. Chu, and Y.-L. Jiang, "Light-Addressed Electrodeposition of Enzyme-Entrapped Chitosan Membranes for Multiplexed Enzyme-Based Bioassays Using a Digital Micromirror Device," *Sensors,* vol. 13, pp. 10711-10724, 2013.

[25] W. mechanically stableLee, C. Y. Bae, S. Kwon, J. Son, J. Kim, Y. Jeong*, et al.*, "Cellular hydrogel biopaper for patterned 3D cell culture and modular tissue reconstruction," *Advanced healthcare materials,* vol. 1, pp. 635-639, 2012.

[26] W. Shang, Y. Liu, W. Wan, C. Hu, Z. Liu, C. T. Wong*, et al.*, "Hybrid 3D printing and electrodeposition approach for controllable 3D alginate hydrogel formation," *Biofabrication,* 2017.

[27] F. Ozawa, K. Ino, Y. Takahashi, H. Shiku, and T. Matsue, "Electrodeposition of alginate gels for construction of vascular-like structures," *Journal of bioscience and bioengineering,* vol. 115, pp. 459-461, 2013.

[28] S. J. Bidarra, C. C. Barrias, M. A. Barbosa, R. Soares, and P. L. Granja, "Immobilization of human mesenchymal stem cells within RGD-grafted alginate microspheres and assessment of their angiogenic potential," *Biomacromolecules,* vol. 11, pp. 1956-1964, 2010.

[29] Z. Liu, M. Takeuchi, M. Nakajima, T. Fukuda, Y. Hasegawa, and Q. Huang, "Batch Fabrication of Microscale Gear-Like Tissue by Alginate-Poly-L-lysine (PLL) Microcapsules System," *IEEE Robotics and Automation Letters,* vol. 1, pp. 206-212, 2016.

[30] Y. T. Matsunaga, Y. Morimoto, and S. Takeuchi, "Molding cell beads for rapid construction of macroscopic 3D tissue architecture," *Advanced Materials,* vol. 23, pp. H90-H94, Mar 25 2011.

[31] T. Sun, Q. Huang, Q. Shi, H. Wang, X. Liu, M. Seki*, et al.*, "Magnetic assembly of microfluidic spun alginate microfibers for fabricating three-dimensional cell-laden hydrogel constructs," *Microfluidics and Nanofluidics,* vol. 19, pp. 1169-1180, 2015.

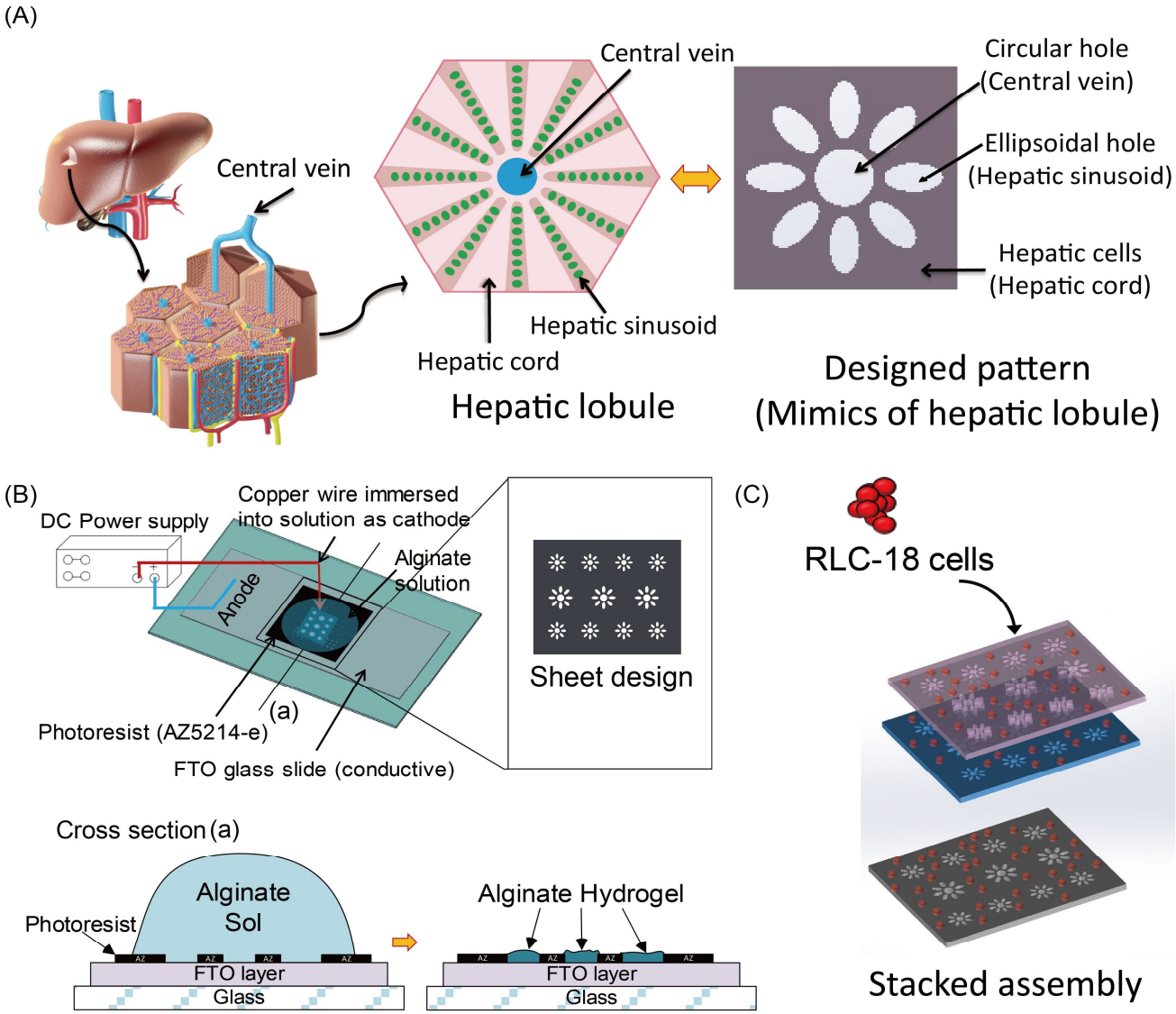

Figure. 1 (A) The structure of the hepatic lobule as the functional units of the liver (left), and the two-dimensional microarchitecture of the hepatic lobule (right). (B) We developed a micro-patterned electrode device using a photolithography technique. Two kinds of hepatic lobule patterns were designed with different outer diameters (1.5 mm and 2.0 mm). A DC voltage was applied to the device to trigger the electrodeposition process. The cross section (a) shows the changes before and after the electrodeposition process. The alginate solution goes through the gelation process to form an alginate hydrogel structure on an FTO layer based on the principle of electrodeposition. (C) The fabricated alginate cell sheets are further detached and stacked to form multi-layered hepatic lobule-like tissue.

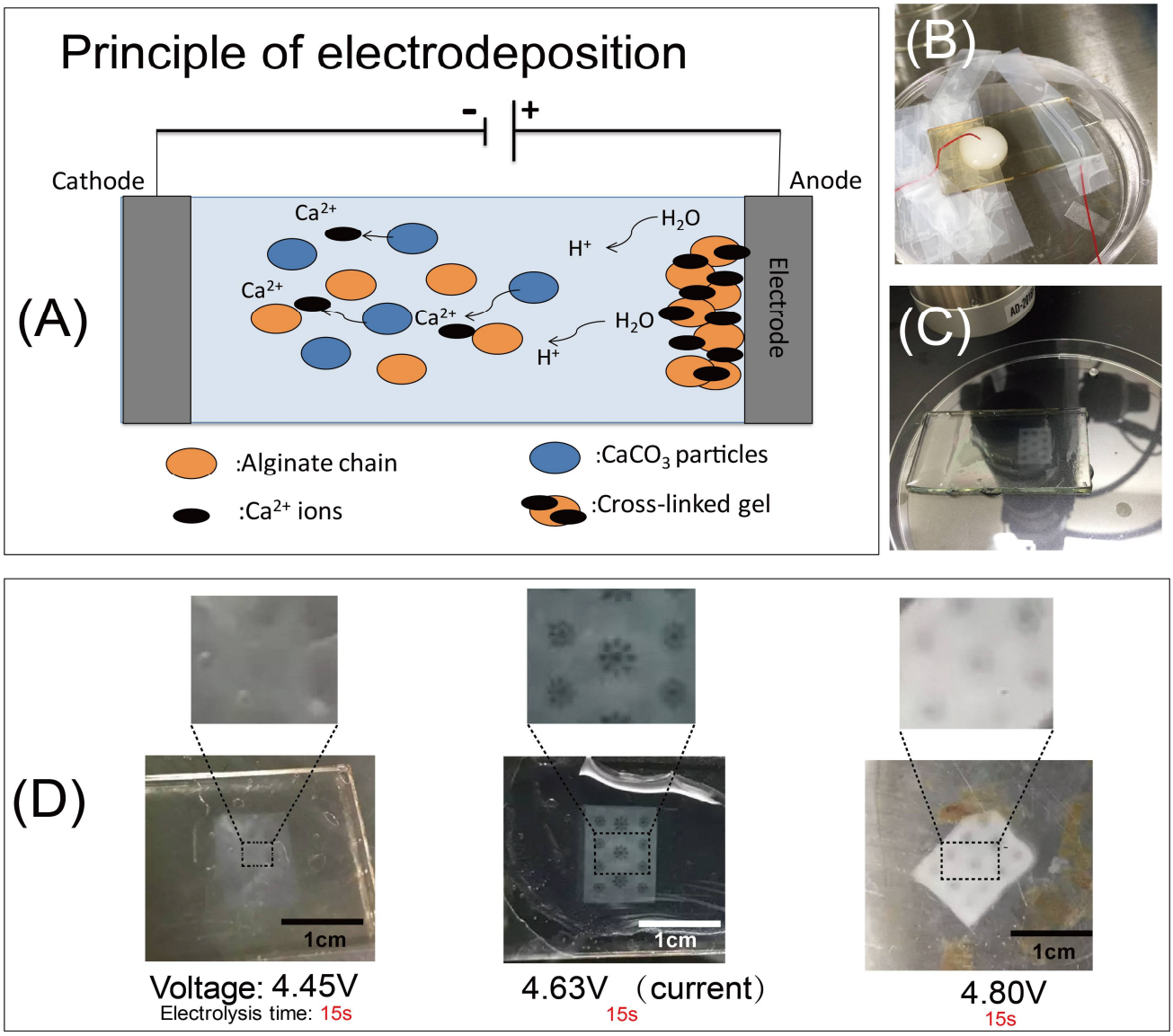

Figure 2 (A) The principle of electrodeposition. (B) The experimental setup before electrodeposition; A DC power supply was utilized to trigger the electrodeposition process by attaching the anode to the FTO glass and immersing the cathode into the deposition solution (Red wire). (C) The Ca-alginate gel sheet was deposited onto the micro-electrode area corresponding to the design. (D) The effect of the applied voltage on the stability of the gel sheet structure. A lower voltage leads to an unstable gel sheet generation due to the insufficient cross-link of Ca-alginate chain (Left image); A higher voltage leads to a thick gel sheet generation without the hepatic lobule pattern due to the diffusion of Ca^{2+} ions (Right image).

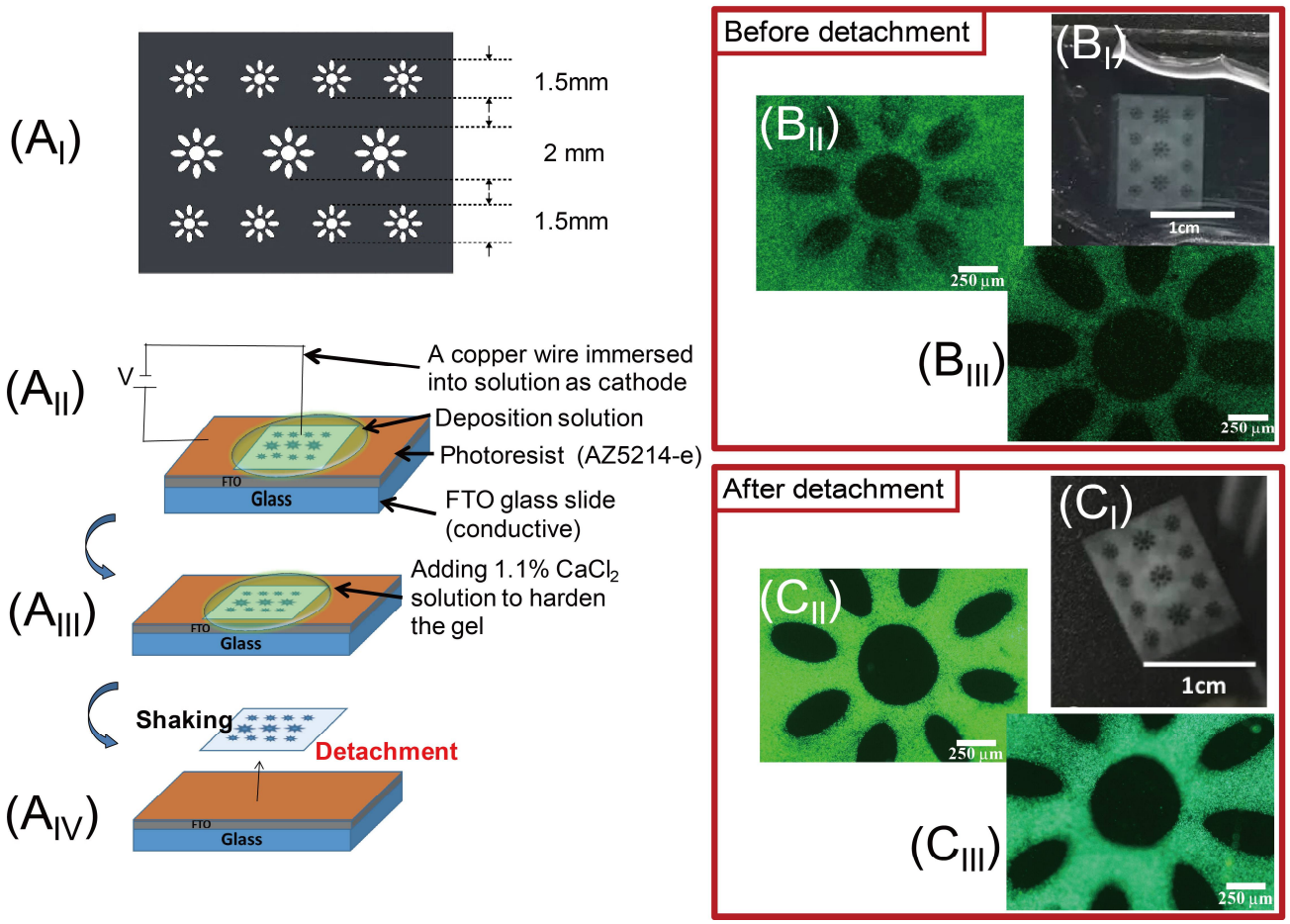

Figure 3 (AI) Two types of hepatic lobule patterns with outer diameters (1.5 mm and 2 mm) were designed. (AII) Ca-alginate gel sheet was deposited onto the micro-electrode area by applying a DC voltage. (AIII) After washing away the non-linked alginate, 1.1% $CaCl_2$ solution was dropped onto the gel sheet to harden the structure. (AIV) After further incubation within culture medium for 24 h, the gel sheet will detach from the substrate by gently shaking. The gel sheet **before** detachment was imaged under an optical (BI) and fluorescence microscope, both with a 1.5 mm and 2 mm diameter (BII and BIII respectively). The gel sheet **after** detachment was imaged under an optical (CI) and fluorescence microscope, both with a 1.5 mm and 2 mm diameter (CII and CIII respectively). The results corresponding to a 1.5 mm diameter were measured to be 1567 $\pm$ 133 µm (n > 10). The results corresponding to a 2 mm diameter were measured to be 2028 $\pm$ 61 µm (n > 4).

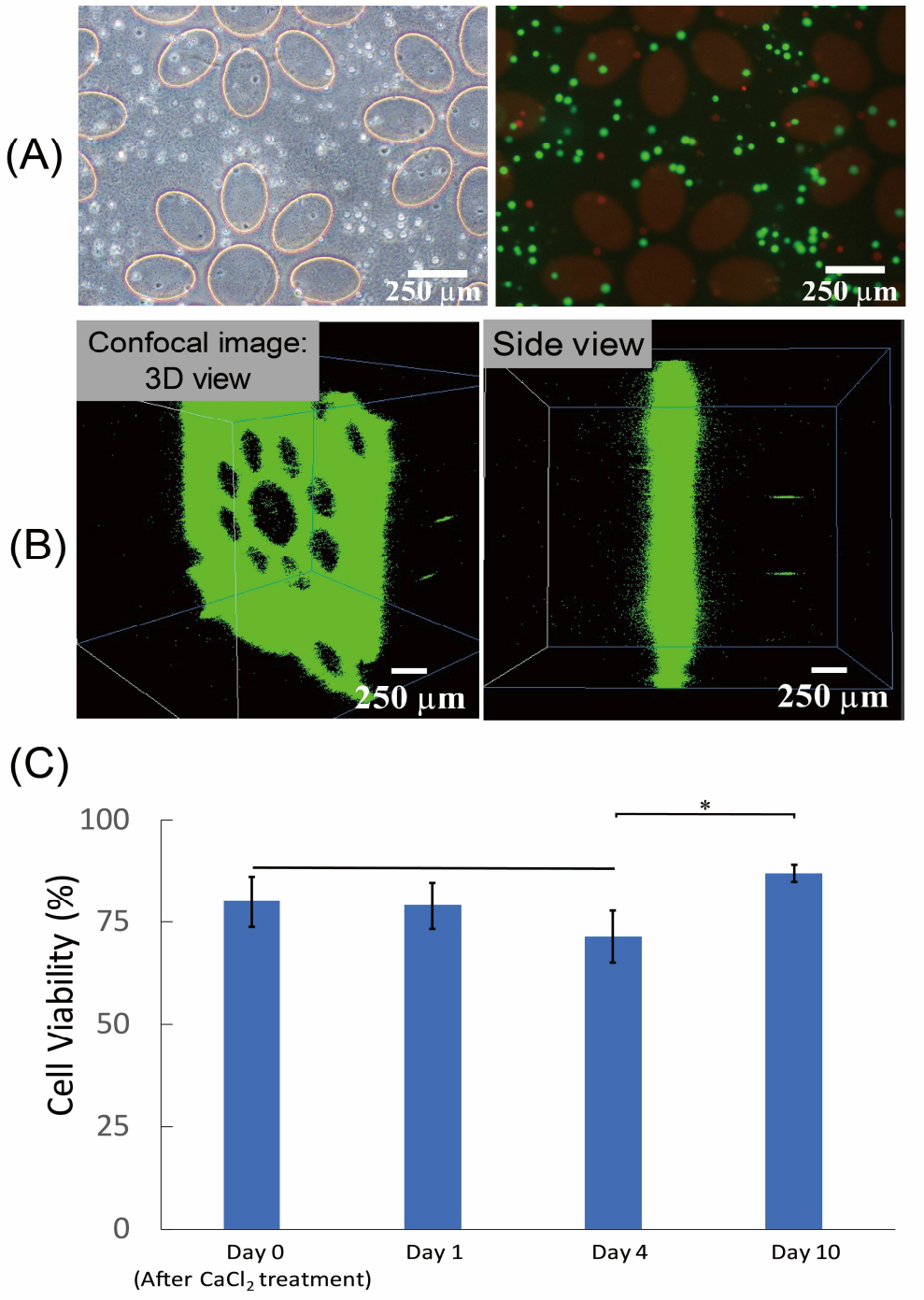

Figure 4. (A) Cell viability soon after electrodeposition on FTO glass was ascertained using light and fluorescence microscopy. Viability was measured to be 80 % by counting the number of live and dead cells. (B) The confocal images show the 3D view of the gel sheet. The height was approximately 302 ± 22 μm (N>3). (note that the patterns used here are old versions) (C) Cell viability was checked after Ca^{2+} treatment (time 0 of the culture), Day 1, Day 4 and Day 10. There is no significant change in cell viability during Day 0, Day 1 and Day 4. Cell viability of Day 10 was significantly upregulated compared with the one of Day 4.

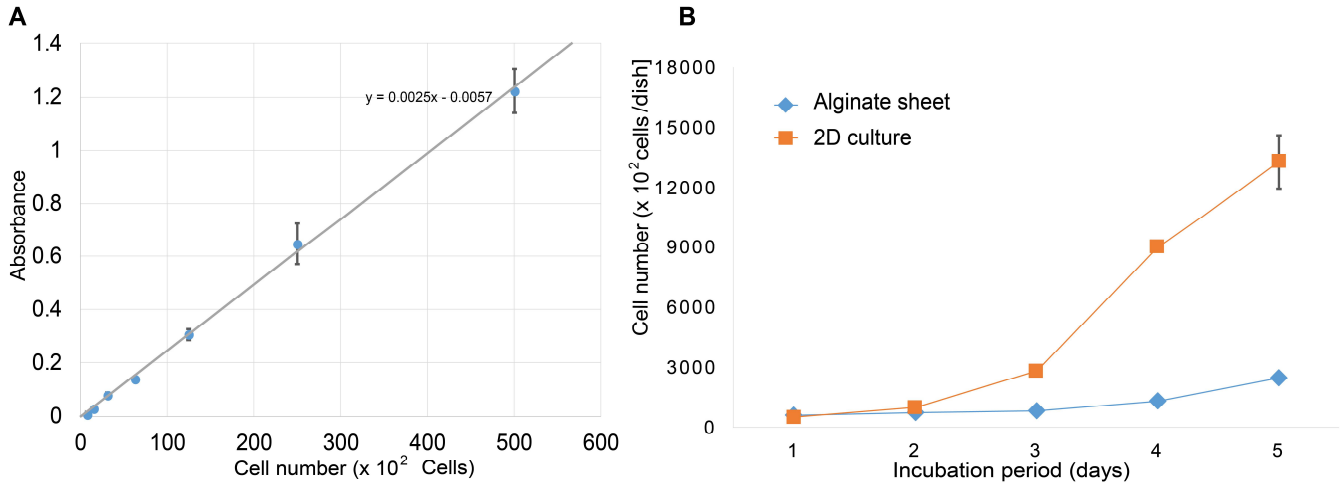

Figure 5. (A) The calibration curve of a linear-fitting model [f(x) = (p1 × x) – 0.0057; p1 = 0.0025] shows the relationship between the RLC-18 cell number and absorbance (OD) using the CCK8 assay. (B) Change in the cell number of the alginate cell sheet and 2D culture group during the incubation period (note that one dish only contained one alginate sheet).

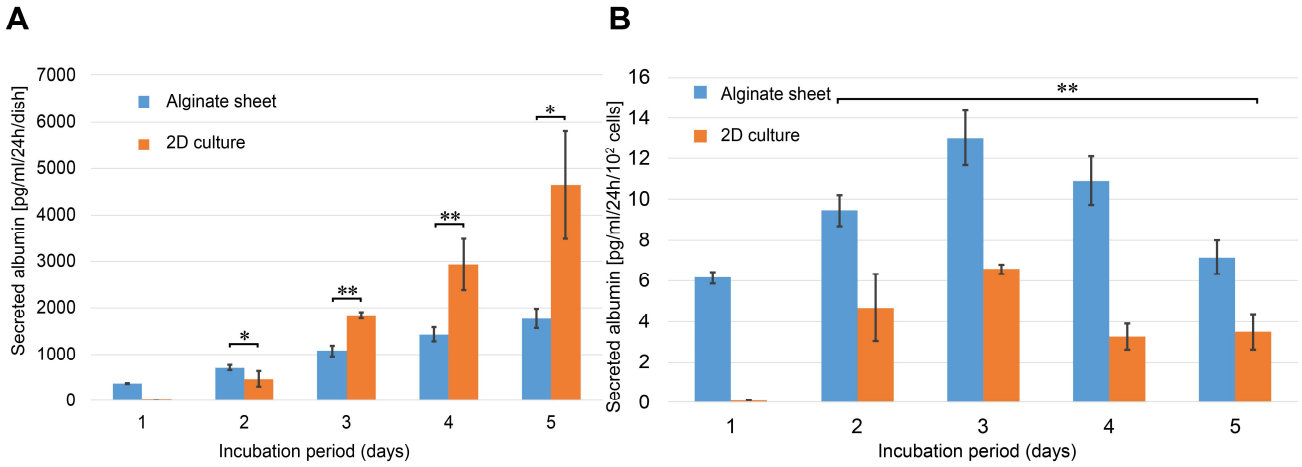

Figure 6. Albumin secretion per dish (A) and per 100 cells (B) of the alginate sheet and 2D culture. Data represent the mean ± standard derivation of at least three experiments from four independent cell preparations. *p < 0.05; **p < 0.01 (note that one dish only contained one alginate sheet).

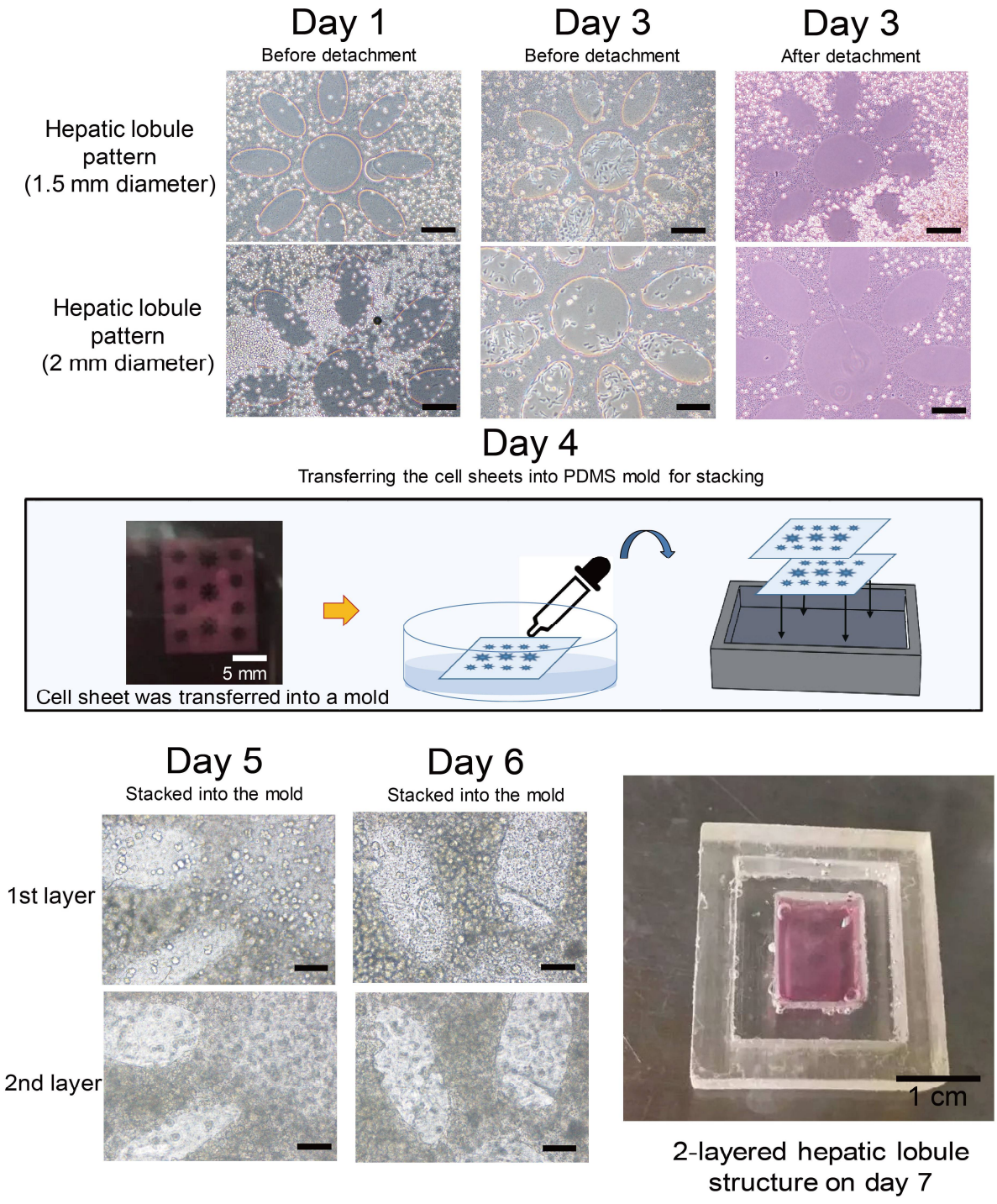

Figure 7. Hepatic lobule patterns of cell sheets on FTO glass was observed under a light microscope on day 1. Hepatic lobule patterns with 1.5 mm and 2 mm diameters were observed before and after detachment on day 3. The fluorescence microscopy image shows cell viability within the cell sheet on day 4; the detached cell sheets were stacked into the PDMS mold to form a 2-layered hepatic lobule model. Light microscopy images show the 1st and 2nd layer of assembled 2-layered hepatic lobule-like model on day 5 and day 6. Scale bars: 250 µm.

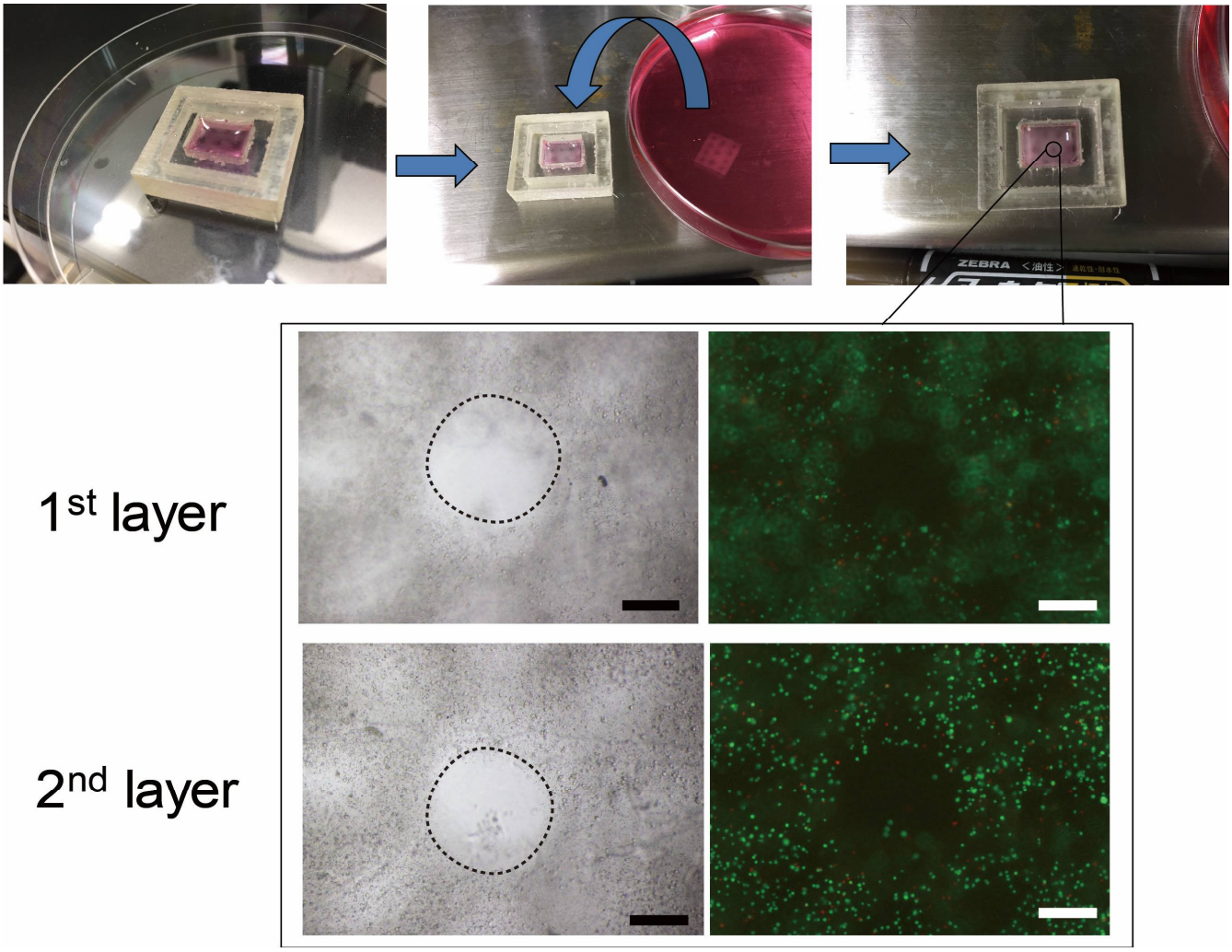

Figure 8. Alginate sheet containing liver cells was assembled into a pre-defined PDMS mode layer by layer to form a 2-layered hepatic lobule-like structure. The optical and fluorescence images of 1st layer and 2nd layer under microscope show that the patterns were aligned during stacking to form an uninterrupted central vein. The circular dash line indicates the inner edge of the alginate cell sheet. The alignment error is less than 200 μm.